[redacted]

Copy 18
NASA TM X-256

[redacted]

NASA TM X-256

# TECHNICAL MEMORANDUM

X-256

## PERFORMANCE CHARACTERISTICS OF A WING-BODY COMBINATION WITH A TWO-DIMENSIONAL EXTERNAL-INTERNAL-COMPRESSION INLET AT MACH 3.5 AND 3.0

By Robert W. Cubbison and Donald O. Barnett

Lewis Research Center
Cleveland, Ohio

CLASSIFIED
To [illegible]
By authority of [illegible]
[illegible] 7-71
[illegible]

LEWIS LIBRARY, NASA
CLEVELAND, OHIO

NATIONAL AERONAUTICS AND SPACE ADMINISTRATION
WASHINGTON July 1960

CLASSIFIED

[redacted]

DECLASSIFIED

NATIONAL AERONAUTICS AND SPACE ADMINISTRATION

TECHNICAL MEMORANDUM X-256

# PERFORMANCE CHARACTERISTICS OF A WING-BODY COMBINATION WITH A TWO-DIMENSIONAL EXTERNAL-INTERNAL-COMPRESSION INLET AT MACH 3.5 AND 3.0*

By Robert W. Cubbison and Donald O. Barnett

## SUMMARY

The overall performance of a flat-bottom wing-body combination in conjunction with a variable-geometry, two-dimensional external-internal-compression inlet was investigated in the Lewis 10- by 10-foot supersonic wind tunnel at Mach numbers of 3.5 and 3.0 with Reynolds numbers, based on body length, of $25.1\times10^6$ and $19.8\times10^6$, respectively. Basic wing-body and inlet performance and the overall aerodynamic characteristics of the complete configuration are presented. Peak lift-drag ratios (L/D) of 7.75 were measured at Mach 3.5 and a Reynolds number of $25.1\times10^6$ with the wing-body configuration alone. Installation of the inlet system reduced the maximum L/D values to 6.9. The inlet bleed drag produced about half of this loss in L/D. Relocating the inlet from the edge to one-fourth of the way into the boundary layer resulted in peak L/D values of about 6.6. At Mach 3.0, the inlet installation decreased the peak wing-body L/D from 7.7 to 6.5. Approximately half of this reduction came from the combination of bleed and spillage drag and half from the boundary-layer diverter system and inlet wave and friction drag.

Inlet performance was favorably influenced by its location in the compression field of the wing and fuselage at angle of attack. Total-pressure recoveries at Mach 3.5 increased from 75 to 84 percent as the angle of attack was increased from $0^\circ$ to $6^\circ$. The corresponding engine mass-flow ratios (based on inlet capture area) were 87 and 105 percent with bleed flows of 8 and 8.5 percent, respectively. At Mach 3.0, maximum total-pressure recoveries of 89.5 percent were measured with 82.5 percent engine mass-flow ratio at $4^\circ$ angle of attack.

*Title, Unclassified.

DECLASSIFIED

DECLASSIFIED



CONFIDENTIAL

## INTRODUCTION

For supersonic bombers and transports, airplane configurations capable of high lift-drag ratios are of considerable importance. Several investigations (e.g., refs. 1 to 3) have been conducted on different types of wing-body combinations. In practice, of course, the aircraft designer is more interested in the performance of a configuration that includes a realistic powerplant and induction system. Therefore, an operating two-dimensional inlet was installed under the flat-bottom, semielliptical fuselage, arrow-wing configuration of reference 1 to determine the overall performance.

E-722

The choice of inlet is influenced by the manner in which the powerplants are to be installed, the mission to be accomplished, and the required speed range. Since high-Mach-number bombers and transports are required to operate over a wide speed range, it is desirable to capitalize on any favorable compression fields produced by the wing and body. The wing-body configuration used herein lent itself readily to the installation of a single two-dimensional high-aspect-ratio inlet located back in the favorable compression field under the wing. The model was then considered representative of a multiengine airplane with six engines installed side by side and fed by a common inlet.

The objective of this study was to determine the aerodynamic characteristics of a high-performance wing-body combination in conjunction with a representative induction system. The overall effect on airplane performance and the basic inlet performance data are presented. The investigation was conducted in the Lewis 10- by 10-foot supersonic wind tunnel at Mach numbers of 3.0 and 3.5, over an angle-of-attack range from $0^{\circ}$ to $6^{\circ}$ and at Reynolds numbers of $19.8\times10^{6}$ and $25.1\times10^{6}$ based on fuselage length.

## SYMBOLS

| | |
|---|---|
| $A$ | area |
| $C_D$ | drag coefficient, $D/q_0S_W$ |
| $C_{D,0}$ | drag coefficient at zero lift angle |
| $dC_D/dC_L^2$ | drag rise factor |
| $C_L$ | lift coefficient, $L/q_0S_W$ |
| $C_{M,0.24\bar{c}}$ | pitching-moment coefficient about the assumed center of gravity, $\mathcal{M}/q_0S_W\bar{c}$ |

DECLASSIFIED

CONFIDENTIAL

DECLASSIFIED



E-722

CL-1 back

| | |
|---|---|
| $C_{M,0}$ | pitching-moment coefficient at zero lift angle |
| $C_{M,\alpha}$ | $dC_M/d\alpha$ |
| $\bar{c}$ | mean aerodynamic chord |
| D | drag |
| h | fuselage boundary-layer diverter height |
| L | lift |
| M | Mach number |
| $\mathcal{M}$ | moment about assumed center of gravity |
| $m/m_0$ | mass-flow ratio, $\rho AV/\rho_0 A_i V_0$ |
| P | total pressure |
| q | dynamic head |
| Re | Reynolds number based on fuselage length |
| $S_W$ | wing area including portion submerged in fuselage, 41.44 sq ft |
| V | velocity |
| $\alpha$ | angle of attack |
| $\delta$ | fuselage boundary-layer thickness |
| $\rho$ | density |

Subscripts:

| | |
|---|---|
| av | average |
| B | bleed |
| i | inlet |
| max | maximum |
| min | minimum |
| 0 | free-stream condition |
| 3 | compressor-face station |



DECLASSIFIED

DECLASSIFIED
CONFIDENTIAL

## APPARATUS AND PROCEDURE

### Wing and Body

The basic wing-body combination was the same as configuration 13 of reference 1. A photograph of the configuration without the inlet is shown in figure 1(a) and with the inlet installed in figure 1(b). Pertinent dimensions are shown in figure 2(a). The fuselage was semi-elliptical in cross section with a flat bottom and a conically tapered forebody canted upwards at $3^{\circ}38'$. The arrow wing, which is essentially a flat plate, was swept back at $73.6^{\circ}$ and had an aspect ratio of 1.72. The canopy-like protrusion on top of the fuselage was necessary to accommodate the sting and balance. A shroud designed to raise the base and balance cavity pressures to near ambient pressure, thus minimizing the tare-force corrections, was mounted just off the fuselage base.

### Inlet Drag Simulator and Fuselage Boundary-Layer Diverter

An inlet drag simulator (fig. 2(b)) was installed to determine the engine-pod friction drag, wave drag, and boundary-layer diverter drag. This device would give the same results that would be obtained with a maximum-capture stream tube entering the inlet when all internal forces of the induction system are subtracted from the balance forces. The simulator was designed so that the wetted area and wedge angles equaled that of the inlet system. The vertical plates of the simulator consisted of both inlet side fairings, and the angle at the leading edge of the horizontal plate matched that of the inlet cowl. The simulator was supported below the fuselage, as was the inlet, by a double-pylon boundary-layer diverter system. A gap was left midway along the length of each pylon strut to prevent choking of the constant-area internal passage. The height of the diverter could be adjusted from 1.75 to 1.25 inches to give $h/\delta$ values of 1.0 and 0.75, respectively, at Mach 3.5 at zero angle of attack.

### Induction System

The inlet, designed for a cruise Mach number of 3.5, was similar to that of reference 4, with the basic difference in the aspect ratio. It was a two-dimensional inlet having isentropic external and internal compression with an aspect ratio (width to cowl-lip height) of 5.64. Details of the aerodynamic design and installation are shown in figures 2(c) and (d). The inlet system was installed under the fuselage on the double-pylon boundary-layer diverter system. The exit of the inlet-engine pod was alined with the fuselage base. The inlet-engine pack was 3.11 feet long and 1.79 feet wide.

DECLASSIFIED
CONFIDENTIAL

DECLASSIFIED
CONFIDENTIAL



As seen in figure 2(d), extensive variable geometry was incorporated in the model. It was possible to move remotely the external ramp, the bypass door, and the internal lip. Because of the width of the inlet, structural considerations dictated the use of dual jacks on each movable piece. The external ramp was variable through a compressive turning angle range of $7^{\circ}$ to $15^{\circ}$. The contour of the front ramp, starting with an initial angle of $5\frac{1}{2}^{\circ}$, was designed to produce isentropic compression focused at the cowl lip from an initial Mach number of 3.5 to a final Mach number of 2.7. Internally, the cowl lip was designed to compress the flow from Mach 2.7 down to a Mach number of 1.5 ahead of the terminal shock. The internal shock system was focused at the leading edge of the internal lip. At the Mach 3.5 design condition the total compressive turning was $45.64^{\circ}$ with $14.4^{\circ}$ external and $16.84^{\circ}$ internal. The low-angle side fairings ($2^{\circ}$ in the streamwise direction) were swept back at the initial shock angle.

E-722

In order to establish supersonic flow in the inlet, the bypass door attached to the trailing edge of the external ramp was opened, and large quantities of air were bypassed around the throat. After supersonic flow was established, the door was closed to the design or flush position. With the door in this position there was a flush slot (approximately 0.65-in. gap) between the door and internal lip for ramp boundary-layer removal. Also, as an alternate configuration, additional provisions were made to have boundary-layer bleed on the side walls and cowl just ahead of the throat. Both of these systems discharged through a low-angle bypass to the free stream.

In addition to the movable front ramp, the internal lip could be used to vary the throat area. At the Mach 3.5 design, the internal lip formed an average-$4^{\circ}$-included-angle subsonic diffuser having a design exit Mach number of 0.53, corresponding to the match condition for a hypothetical low-pressure-ratio, high-weight-flow turbojet engine. Transition from square corners at the throat to rounded corners at the compressor-face station was accomplished by filleting on both the internal lip and the bottom plate. The terminal shock in the main duct was positioned by the mass-flow control ramp that controlled the throat area of a convergent-divergent nozzle. This system was incorporated to reduce the amount of internal axial force exerted on the balance. Similarly, the bleed flow was ducted back through the upper passage and metered through another convergent-divergent nozzle. The bleed duct was always operated supercritical by positioning the shock with the bleed control ramp. Changes in the amount of bleed were made with the internal lip by moving it into the local stream creating, in effect, a combination flush slot and ram scoop.

DECLASSIFIED
CONFIDENTIAL

DECLASSIFIED
CONFIDENTIAL

The details of the modified bleed system used to document the inlet performance at Mach 3.0 are shown in figure 2(c). Because of the existing sting-support system of the wing-body combination, the axial bleed discharge area was too small for operation at Mach 3.0. Sufficient additional bleed exit area was added by venting the bleed passage into the boundary-layer diverter and opening the cowl bleed. The following symbology is presented to define the various configurations:

| Symbol | Configuration |
|---|---|
| B | Body |
| WB | Wing + Body |
| WBS | Wing + Body + Wetted Area Simulator |
| $WBI_{1.0}$ | Wing + Body + Inlet with $h/\delta = 1.0$ |
| $WBI_{0.75}$ | Wing + Body + Inlet with $h/\delta = 0.75$ |

E-722

## Data Reduction

A flow survey ahead of the inlet was made with static- and total-pressure instrumentation to determine the Mach number and boundary-layer thickness at the inlet station (station i). A three-component electrical-strain-gage balance was used to measure model forces. All measurements were corrected for fuselage-base and balance-cavity forces. Also, for configuration WBS, the base forces of the vertical and horizontal plates were accounted for. In the inlet tests, the change in total momentum of the captured mass flow from free stream to the model exit was subtracted from the force measurements. In all cases, the main-duct momentum change was accounted for; however, data are presented with and without bleed-drag corrections. All aerodynamic coefficients and bleed-drag coefficients are referenced to the wing area, including the portion submerged in the fuselage. The moment coefficient was calculated about the 0.24 $\bar{c}$ point, the assumed center-of-gravity location.

The engine and bleed mass-flow ratios presented are referenced to inlet capture area ($m_0 = \rho_0 V_0 A_i$). Locations of pressure instrumentation are shown in figure 2(c). Main-duct total-pressure recovery was calculated from an area-weighted average of 18 tubes at the compressor-face station (17.57). Mass-flow ratios in both the main and bleed ducts were calculated from total pressure and the calibrated choked nozzles with

DECLASSIFIED
CONFIDENTIAL

DECLASSIFIED
CONFIDENTIAL



the assumption of one-dimensional isentropic flow between the measuring and throat stations. The total pressures were measured at stations 24.9 and 28.5 in the main and bleed ducts, respectively. Calculations of the flow conditions at the nozzle exits were made with the assumption of one-dimensional isentropic flow between the nozzle throats and exits and a calibration of the exit area. Assumed nozzle-flow coefficients of 0.97 and 0.985 for the main and bleed ducts, respectively, were used in all calculations. The experimental investigation was conducted in the Lewis 10- by 10-foot supersonic wind tunnel at Mach numbers of 3.5 and 3.0 and Reynolds numbers, based on fuselage length, of $25.1\times10^6$ and $19.8\times10^6$, respectively. During the tests the angle of attack was varied from $0^\circ$ to $6^\circ$.

E-722

## RESULTS AND DISCUSSION

### External Performance

Basic aerodynamic data for the body alone, wing and body, and the wing-body and simulator configurations are presented in figure 3 for Mach numbers of 3.5 and 3.0 at Reynolds numbers of $25.1\times10^6$ and $19.8\times10^6$, respectively, based on fuselage length.

Data for the body alone indicate that the flat-bottom fuselage is a rather efficient lifting device, producing a maximum lift-drag ratio in excess of 5.0 at both free-stream Mach numbers. Installing the wing increased the $L/D$ to about 7.75 at Mach 3.5 and approximately 7.7 at Mach 3.0. Addition of the simulator to configuration WB resulted in the loss of about 0.5 and 0.6 in maximum lift-drag ratio at Mach 3.5 and 3.0, respectively.

Adding the inlet drag simulator to the basic wing-body combination increased the lift coefficient at a given angle of attack. However, a net decrease in $L/D$ occurred with the accompanying rise in drag coefficient at both free-stream Mach numbers. The increase in drag was due primarily to the fuselage boundary-layer diverter. The wave-drag component of the simulator is necessarily small because of the low cowl-lip and side-fairing angles. Also, the increase in friction drag is small because of the relatively small increase in wetted area compared with the wing-body combination. As expected, there was an increase in $C_{D,0}$ from configuration WB to WBS; however, the drag rise factor $dC_D/dC_L^2$ remained the same. The longitudinal stability $C_{M,\alpha}$ was unchanged, but $C_{M,0}$ was increased negatively when the simulator was added.

The effect of an operating inlet on the overall performance is presented in figure 4 for configurations $WBI_{1.0}$ and $WBI_{0.75}$ at Mach 3.5

DECLASSIFIED
CONFIDENTIAL

DECLASSIFIED
CONFIDENTIAL

and for configuration $WBI_{1.0}$ at Mach 3.0. Lift-drag ratios at Mach 3.5 are presented including and excluding the inlet bleed drag. Maximum values of 7.3 were obtained with configuration $WBI_{1.0}$ without bleed drag, and 6.9 with bleed drag. Reducing the boundary-layer diverter height from an $h/\delta$ of 1.0 to 0.75 caused a reduction of 0.3 in peak lift-drag ratios. Compared with configuration $WBI_{1.0}$, instrumentation in the central passage of the boundary-layer diverter system showed that configuration $WBI_{0.75}$ produced a greater reduction in the supersonic Mach number in both the front and rear portions of the passage with the attendant larger momentum change.

E-722

Configurations $WBI_{1.0}$ and $WBI_{0.75}$ produced greater lift and drag coefficients than those of configuration WBS. This increase in both coefficients is due to spillage over the cowl lip. Flow spillage was a consequence of the reduced Mach number ahead of the Mach 3.5 design inlet. Local Mach number, of course, is a function of the angle of attack. The inlet installation having an $h/\delta$ of 1.0 did not change the longitudinal stability characteristics other than a decrease in $C_{M,0}$ compared with WBS. Only a slight change occurred when the diverter height was reduced. The drag coefficient at zero lift angle ($C_{D,0}$) was essentially the same for WBS and $WBI_{1.0}$ when all internal forces were accounted for; however, there was a reduction in the drag rise factor. This type of inlet installed underneath the body near the base also should have a favorable effect on the directional stability.

The Mach 3.0 inlet system as described in the apparatus section did not incorporate an optimized bleed system. However, it is felt that the performance data on both the wing-body and inlet configurations are fairly representative of off-design inlet operation. The maximum lift-drag ratio obtained was 6.45 because of the increase in $C_{D,0}$. In general, the same trends occur at Mach 3.0 as at Mach 3.5. Because of increased spillage and bleed flows, $C_{D,0}$ increased about 0.001, compared with configuration WBS, with no change in the drag rise factor. The longitudinal stability was improved slightly.

A comparison of peak lift-drag ratios is presented in figure 5. The body alone at Mach 3.5 produced a peak lift-drag ratio of 5.3. Addition of the wing increased the peak L/D to 7.75. The fuselage boundary-layer diverter drag plus inlet wave and friction drag caused a 0.45 decrement in peak lift-drag ratio. Replacing the simulator with an operating inlet resulted in an additional loss of 0.38 in L/D because of the bleed discharge drag. Finally, a comparison of $WBI_{1.0}$ and $WBI_{0.75}$ shows that a 25-percent reduction in diverter height caused an additional loss in L/D of about 0.3. At Mach 3.0 a total reduction from a peak lift-drag ratio of 7.7 to 6.5 was measured. The combination of spillage

CONFIDENTIAL
DECLASSIFIED

and bleed drag caused about half of the loss in L/D. The other half was due to the diverter, wave, and friction drag.

## Inlet Performance and Its Effect on Overall Performance

A survey ahead of the inlet was conducted to determine the nature of the flow field under the body. Measurements indicated this flow field was nearly two-dimensional; for example, the inlet-station Mach number was reduced from the free-stream value of 3.46 to 3.22, compared with the theoretical value of 3.21 at $4^{\circ}$ angle of attack. A plot of boundary-layer thickness against angle of attack is presented in figure 6. The trend of decreasing thickness with increasing angle of attack can be readily seen. Schlieren photographs presented in figure 7 also indicate this trend. At zero angle of attack the boundary-layer thickness was about equal to the diverter height. As the angle of attack was increased, the Mach number ahead of the inlet and the boundary-layer height were reduced. At a free-stream Mach number of 3.5 and $4^{\circ}$ angle of attack, the inlet $h/\delta$ increased to about 1.1 with further increases at higher angles.

The favorable effects on inlet mass-flow pressure-recovery characteristics created by the wing-body combination can be seen in figure 8. All the mass-flow ratios presented were referenced to inlet capture area ($m_0 = \rho_0 V_0 A_i$). The performance characteristics of configuration $WBI_{1.0}$ are presented in figure 8(a). Maximum engine mass-flow ratios increased from 87 to about 105 percent as the angle of attack was increased from $0^{\circ}$ to $6^{\circ}$. Analysis of the shock structure shows spillages ranging from approximately 5 percent at $4^{\circ}$ to 9 percent at $6^{\circ}$ angle of attack at the design Mach number of 3.5. The total-pressure recovery also increased with increasing angle, the largest increases occurring between $0^{\circ}$ and $4^{\circ}$. Peak recoveries of 82 percent were obtained at $4^{\circ}$ angle of attack (near maximum L/D angle) with 8-percent internal-ramp bleed flow and engine mass flows of 97.5 percent. Zero-angle-of-attack recovery was 0.75. Variations in bleed and critical engine mass-flow ratios were made by moving the external ramp and internal lip. A varying degree of ram scoop could be superimposed on the flush slot by adjusting the internal lip. Optimum or near-optimum internal and external performance at Mach 3.5 could be achieved with two ramp settings of $14.4^{\circ}$ or $14.8^{\circ}$ and either a flush slot or a combination of flush and ram-scoop bleed.

The corrected-weight-flow line shown in figure 8(a) was calculated for critical operation of configuration $WBI_{1.0}$ for $5^{\circ}$ angle of attack (maximum L/D). Provided the induction system can be sized to match an engine at $\alpha$ of $5^{\circ}$ without penalties in recovery or mass-flow, it is shown that critical inlet operation can be maintained at attack angles of $4^{\circ}$, $5^{\circ}$, and $6^{\circ}$. At zero angle of attack, supercritical operation

DECLASSIFIED
CONFIDENTIAL

would result. Relatively high bleed drags in the order of 5 percent of total drag were measured with configuration $WBI_{1.0}$ at maximum lift-drag ratios. This resulted from the large momentum changes due to low total-pressure recoveries in the bleed passage. During the inlet study, a four-wall throat bleed was installed. The data are not presented; however, the results indicated a reduction of about 4 percent in recovery due to the cowl bleed opening being located ahead of the terminal shock. This was accompanied by higher bleed flows with their attendant higher drag.

The minimum distortions of 20 percent measured at the compressor-face station were caused by the short diffuser section and the high matching Mach number ($M_{compressor\ face} = 0.53$). Total-pressure contours typical of all critical inlet operations are shown in figure 9. The flow was generally symmetrical with no localized regions of high or low pressures and with characteristic boundary-layer lobes located in the corners. Since the inlet system was designed for six hypothetical low-pressure-ratio, high-weight-flow engines mounted side by side in the pod, a relatively high distortion level can be reduced by overdiffusing and reaccelerating the flow ahead of the inlet face (ref. 5). With this type of engine installation, this method could be accomplished by placing individual bellmouths ahead of the individual compressors.

Performance data for configuration $WBI_{0.75}$ are presented in figure 8(b). A comparison of these results with configuration $WBI_{1.0}$ shows that a 25-percent reduction in diverter height lowered the total-pressure recovery from 82 to 79 percent at $4^{\circ}$ angle of attack. Also a 0.01 and 0.0002 increase in bleed mass-flow ratio and bleed-drag coefficient, respectively, accompanied the reduction in recovery. The minimum distortion was approximately 5 percent higher. Generally, the same operational trends with corrected weight flow can be seen with this configuration as with $WBI_{1.0}$ if the inlet size is changed to match the corrected weight flow shown on the curves.

The data on the modified configuration $WBI_{1.0}$ for Mach 3.0 operation are presented in figure 10. Bleed mass-flow ratios and drags were not measured because of the changes made in the bleed system. The same favorable effect on inlet characteristics from flow precompression is apparent; however, the trend with angle of attack was more gradual than at Mach 3.5. A peak recovery of 89.5 percent was obtained with 82.5 percent engine mass-flow ratio at $4^{\circ}$ angle of attack. The small range of subcritical operation shown was possible because of the type of bleed system used. Minimum distortions of 24 percent were measured at the compressor-face station for the peak recovery condition. The distortion at Mach 3.0 was considerably higher compared with Mach 3.5 and at all corresponding angles other than $6^{\circ}$. The same procedure

DECLASSIFIED
CONFIDENTIAL

was used to calculate the corrected weight flow shown in figure 9 as was used for Mach 3.5. At an angle of attack of $6^{\circ}$, the inlet would operate slightly subcritical, while at the lower angles critical operation could be maintained.

The effects of bleed mass-flow ratio on both lift-drag ratio and inlet recovery are shown in figure 11. All data are for critical inlet operation, and the lift-drag ratios are presented including and excluding the bleed drag. In general, there was a slight decrease in the lift-drag ratios with bleed drag as the amount of bleed was increased, and the largest effect occurred at $5^{\circ}$ angle of attack. When the bleed drag is removed from the force measurements, the values of lift-drag ratio should be constant with bleed flow as the fairings indicate. Also, the values including the bleed drag should approach those excluding it as the bleed mass flow is reduced, and should be equal at $m_B/m_0 = 0$. Generally speaking, the data show this trend quite well. Other than at zero angle of attack the data show the inlet system produces near optimum recovery over a broad range of bleed flows. Peak recoveries were usually obtained between 8- and 10-percent bleed mass-flow ratios.

From the breakdown of the drag values shown in figure 12, the largest gains for a given wing-body combination can be made by alleviating the boundary-layer diverter drag. The combination of diverter, friction, and wave drag of this configuration represents about 14 percent of the total drag at peak lift-drag ratios. Appropriate design modifications to the inlet system would remove the spillage drag. Although supersonic axial discharge is the most efficient way to bypass flow, improvements in the bleed-passage total-pressure recovery could yield some significant gains in overall performance, since the bleed-drag component was about 5 percent of the total drag.

## CONCLUSIONS

In this investigation an attempt was made to ascertain the overall performance characteristics of a high-performance Mach 3.5 airplane. An arrow-wing, flat-bottom configuration was coupled with a two-dimensional external-internal-compression inlet mounted beneath the fuselage and supported out of the local boundary layer by two pylon struts. Both the wing-body configuration and the inlet system were by themselves capable of high performance. The combination of the two was considered representative of a multiengine airplane with six engines installed side by side and fed by a common inlet.

The experimental study was conducted in the Lewis 10- by 10-foot supersonic wind tunnel at Mach numbers of 3.5 and 3.0. The following significant results were obtained:

DECLASSIFIED CONFIDENTIAL

1. A maximum lift-drag ratio of 7.75 was obtained at a free-stream Mach number of 3.5 and a Reynolds number of $25.1 \times 10^6$ for the wing-body combination. The maximum lift-drag ratio was reduced to 6.9 when the inlet system was installed, with half of the loss attributed to the inlet bleed system.

2. Peak total-pressure recoveries of 0.82 were measured at a Mach number of 3.5 and an angle of attack of $4^{\circ}$. At the same time, the engine mass-flow ratio was 0.975 and bleed mass-flow ratio was 0.08. At zero angle of attack, the peak total-pressure recovery was 0.75.

3. A peak recovery of 0.895 was realized at an engine mass-flow ratio of 0.825 for a Mach number of 3.0 and $4^{\circ}$ angle of attack.

4. Lowering the boundary-layer diverter height from an $h/\delta$ of 1.0 to 0.75 caused a reduction of 0.03 in recovery and a decrease of 0.3 in lift-drag ratio.

These results indicate a high level of performance for both the wing-body - inlet combination and the inlet, and show the advantage of installing the induction system in the favorable compression field under the lifting surfaces. The model used in this study did not provide an adequate bypass system for off-design speeds below Mach 3.0. The bleed system used at Mach 3.0 was not optimized for its effect on overall performance; however, the results are considered representative.

Lewis Research Center
National Aeronautics and Space Administration
Cleveland, Ohio, March 7, 1960

E-722

## REFERENCES

1. Dryer, Murray, and Luidens, Roger W.: Aerodynamic Characteristics of Several Flat-Bottom Configurations at Mach 3.0 and 3.5. NASA MEMO 1-2-59E, 1959.

2. Dryer, Murray, and Luidens, Roger W.: Aerodynamic and Inlet-Flow-Field Characteristics at a Free-Stream Mach Number of 3.0 for Airplanes with Circular Fuselage Cross Sections and for Two-Engine Locations. NACA RM E57K26, 1958.

3. Mueller, James N., and Grimaud, John E.: A Wind-Tunnel Investigation to Evaluate the Aerodynamic Performance of Three Different Airplane Configurations Having Arrow- and Delta-Wing Plan Forms at a Mach Number of 2.91. NASA MEMO 3-11-59L, 1959.

DECLASSIFIED CONFIDENTIAL

DECLASSIFIED
CONFIDENTIAL



4. Connors, James F., and Anderson, Leverett A., Jr.: A Two-Dimensional External-Internal-Compression Inlet with Throat Bypass at Mach 3.05. NASA MEMO 10-3-58E, 1958.

5. Piercy, Thomas G., and Klann, John L.: Experimental Investigation of Methods of Improving Diffuser-Exit Total-Pressure Profiles for a Side-Inlet Model at Mach Number 3.05. NACA RM E55F24, 1955.

E-722

DECLASSIFIED
CONFIDENTIAL

DECLASSIFIED
CONFIDENTIAL

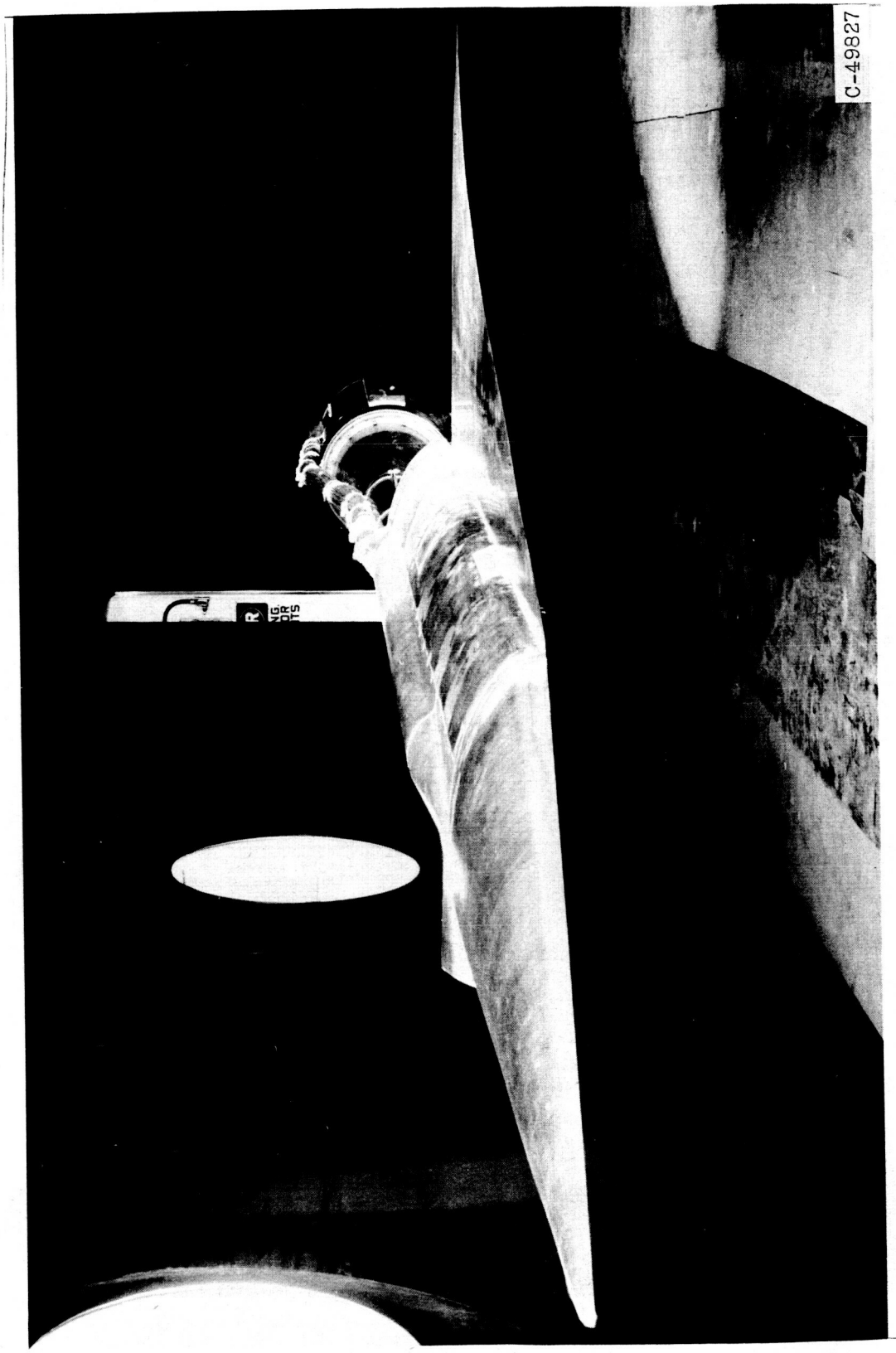


(a) Wing-body combination.

Figure 1. - Model installed in tunnel.

E-722

DECLASSIFIED
CONFIDENTIAL

DECLASSIFIED
CONFIDENTIAL


E-722

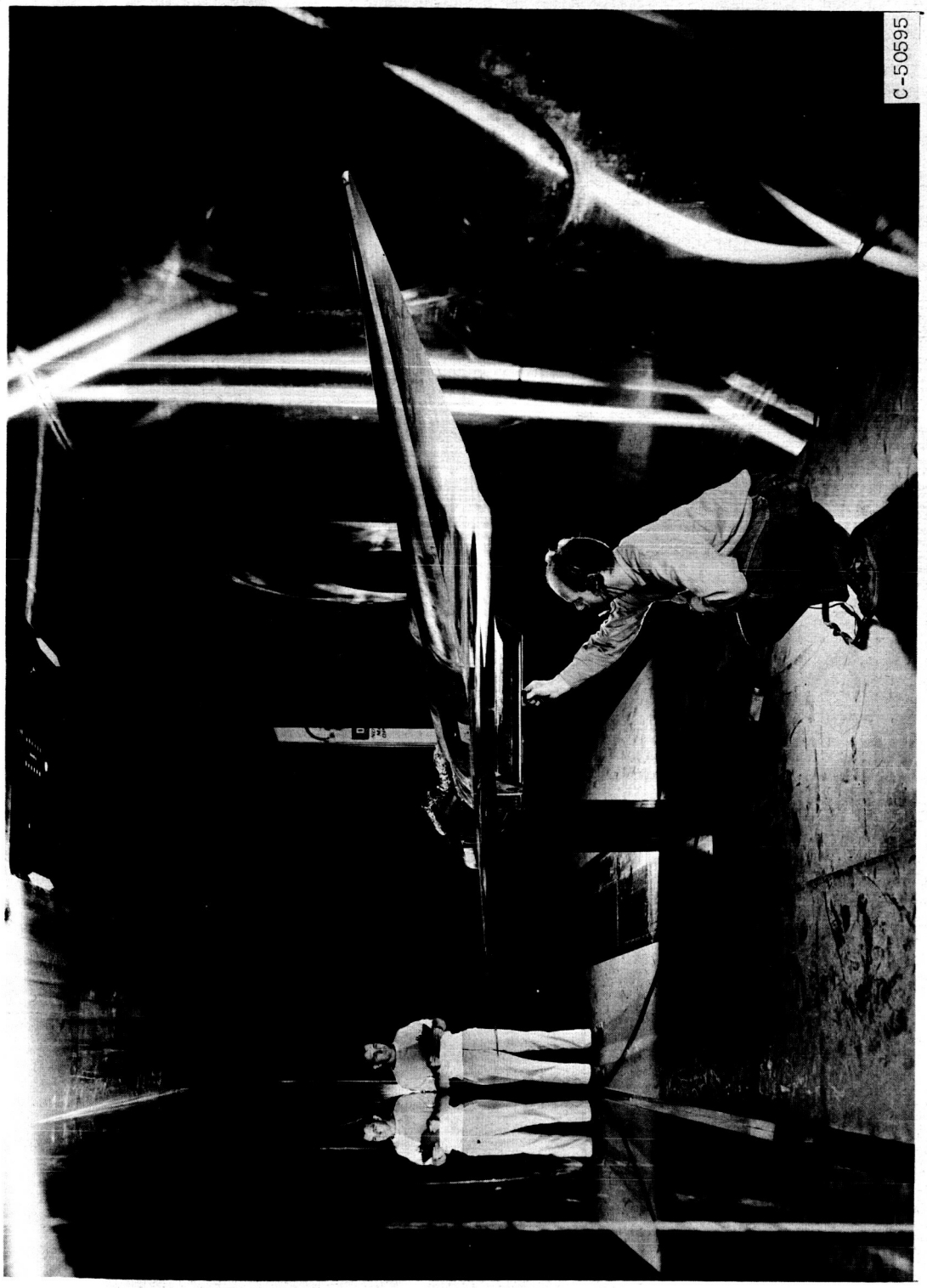


(b) Wing-body with inlet.

Figure 1. - Concluded. Model installed in tunnel.

DECLASSIFIED
CONFIDENTIAL

DECLASSIFIED

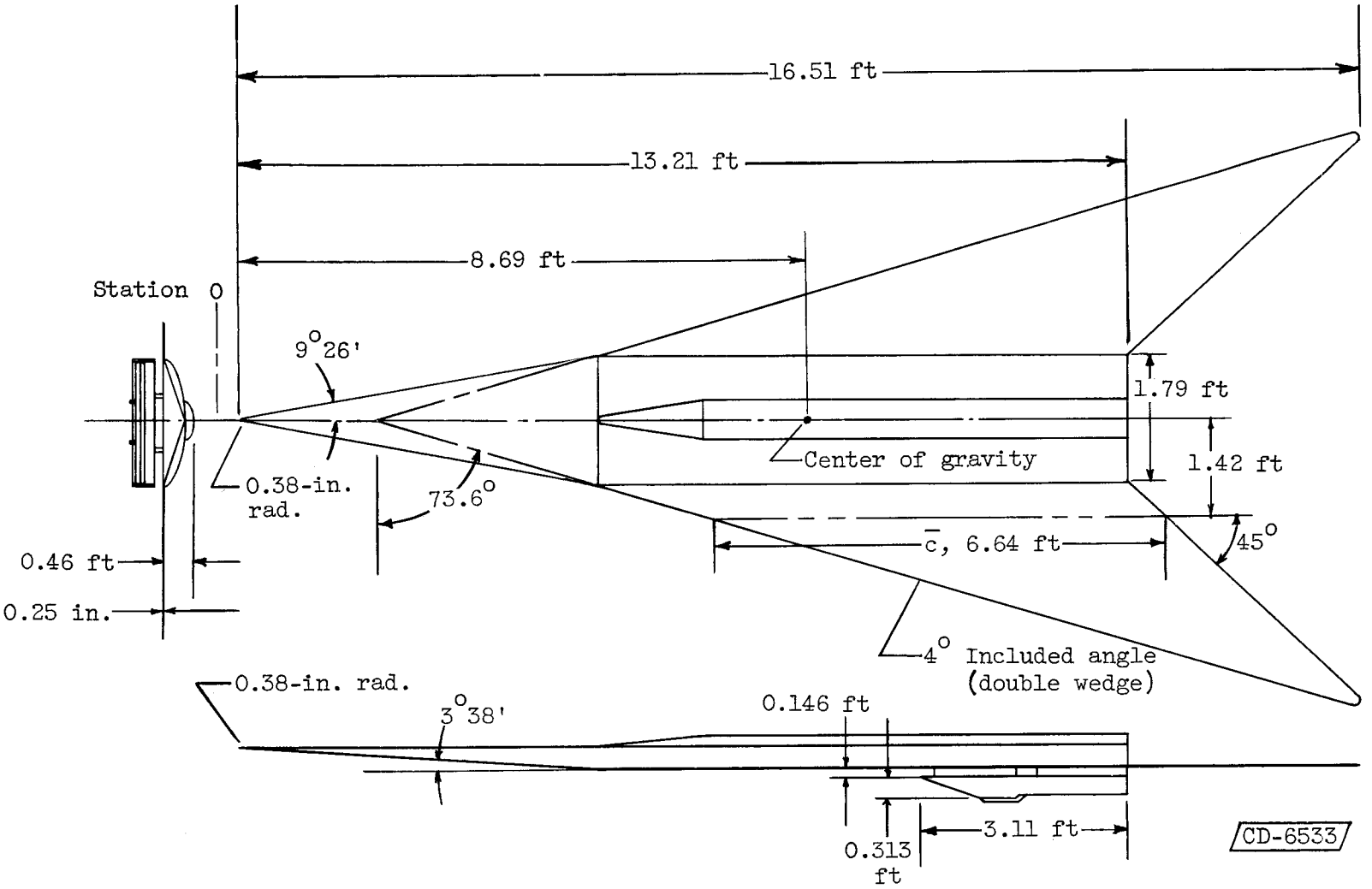


(a) Schematic drawing of model.

Figure 2. - Airplane and inlet details for Mach 3.5 design.

DECLASSIFIED

DECLASSIFIED
CONFIDENTIAL

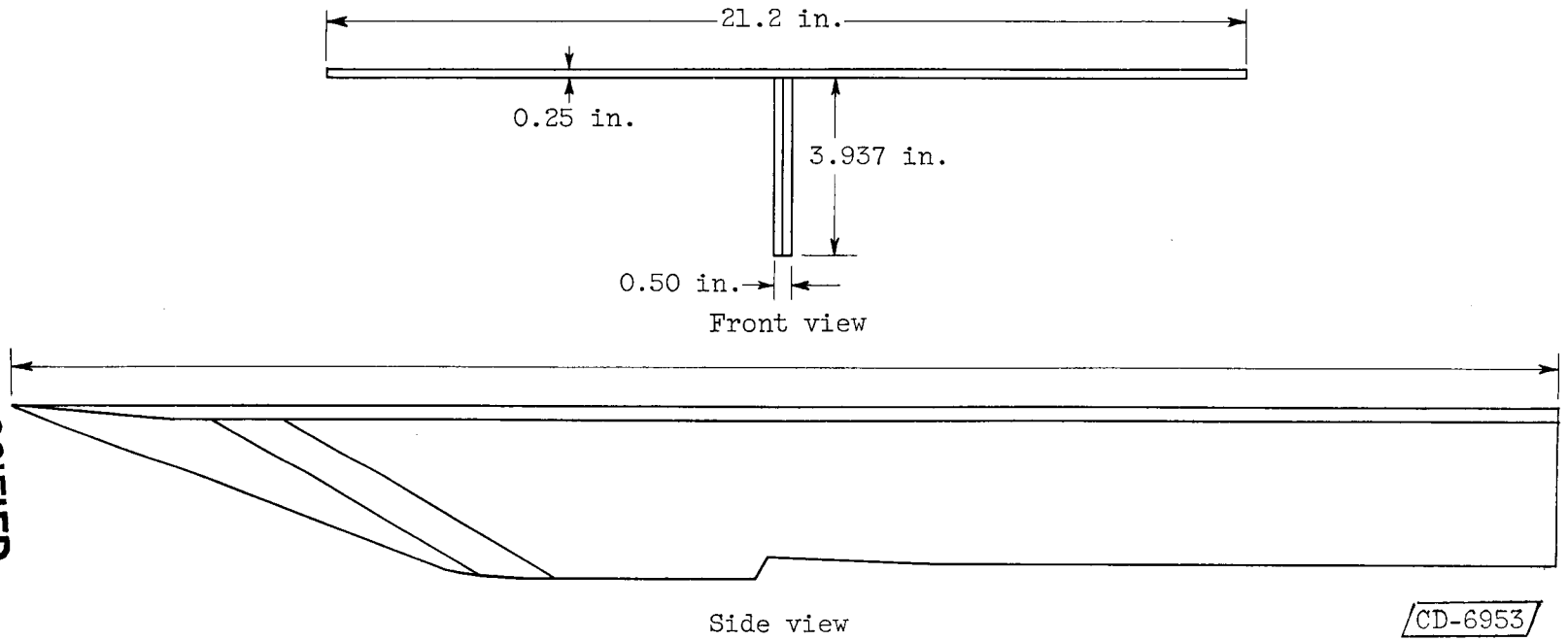


(b) Inlet drag simulator.

Figure 2. - Continued. Airplane and inlet details for Mach 3.5 design.

DECLASSIFIED
CONFIDENTIAL

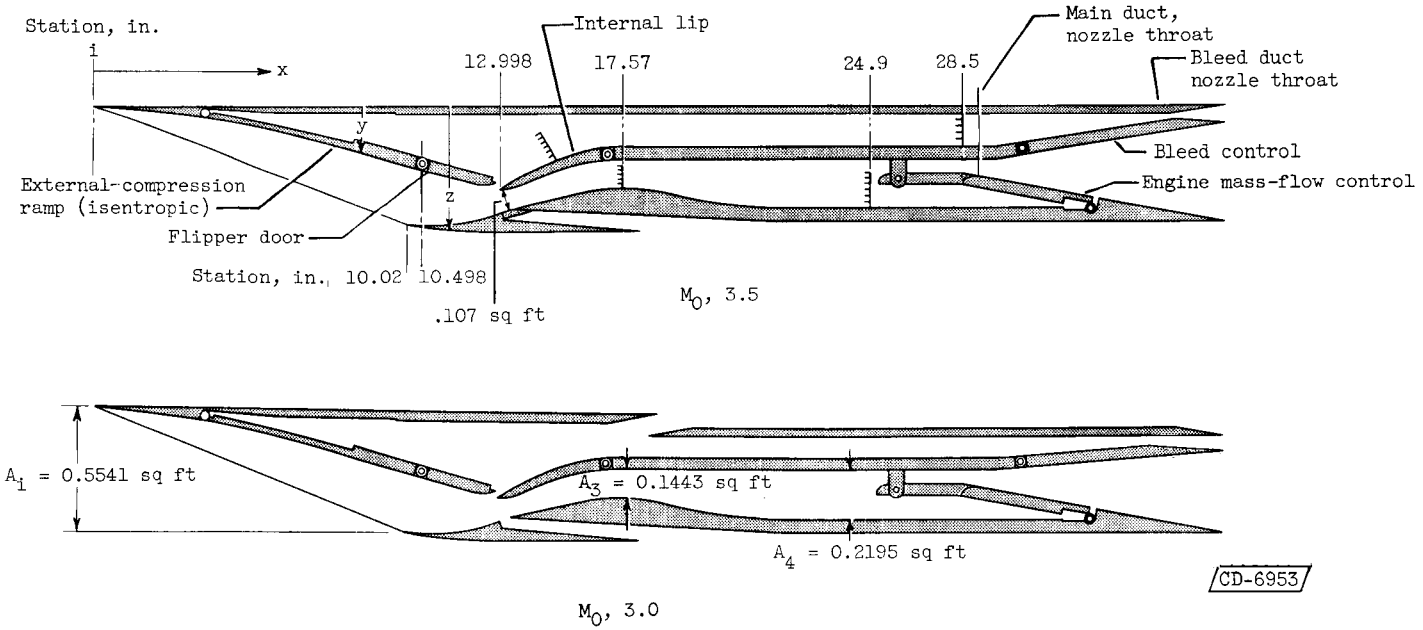


| x,in. | y,in. | x,in. | y,in. | z,in. |
|---|---|---|---|---|
| 0 | 0 | 7.500 | 1.252 | |
| 1.918 | 0.177 | 8.000 | 1.384 | |
| 2.500 | .233 | 8.500 | 1.512 | |
| 3.000 | .290 | 9.000 | 1.636 | |
| 3.500 | .357 | 9.500 | 1.767 | |
| 4.000 | .432 | 10.020 | 1.906 | 3.760 |
| 4.500 | .526 | 10.498 | 2.030 | 3.760 |
| 5.000 | .628 | 11.000 | Bypass | 3.760 |
| 5.500 | .737 | 11.500 | door & | 3.730 |
| 6.000 | .854 | 12.000 | bleed | 3.674 |
| 6.500 | .985 | 12.500 | gap | 3.561 |
| 7.000 | 1.120 | 12.998 | 2.651 | 3.422 |

(c) Inlet aerodynamic details.

Figure 2. - Continued. Airplane and inlet details for Mach 3.5 design.

E-722

CL-3 back

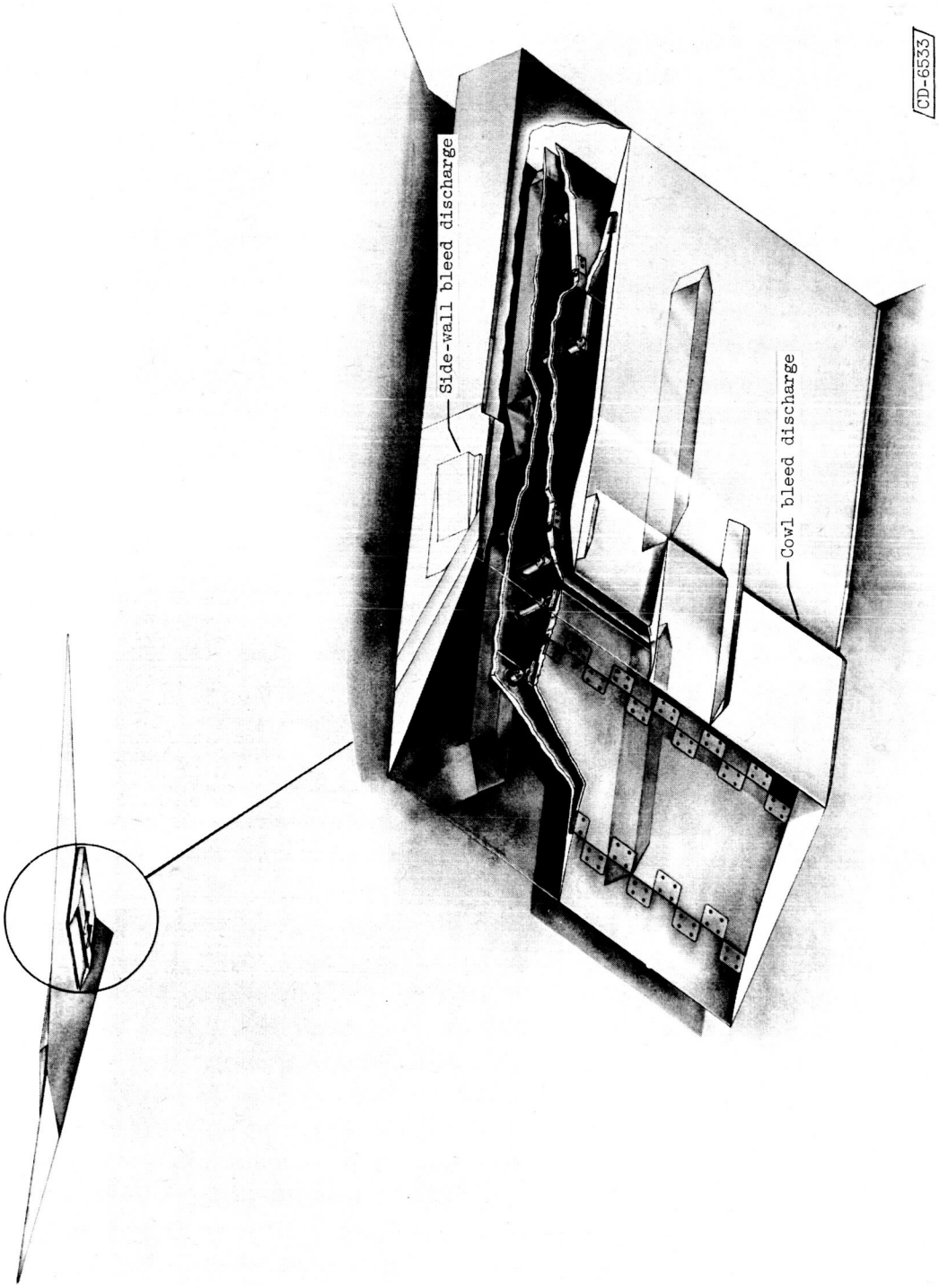


(d) Inlet installation.

Figure 2. - Concluded. Airplane and inlet details for Mach 3.5 design.

DECLASSIFIED

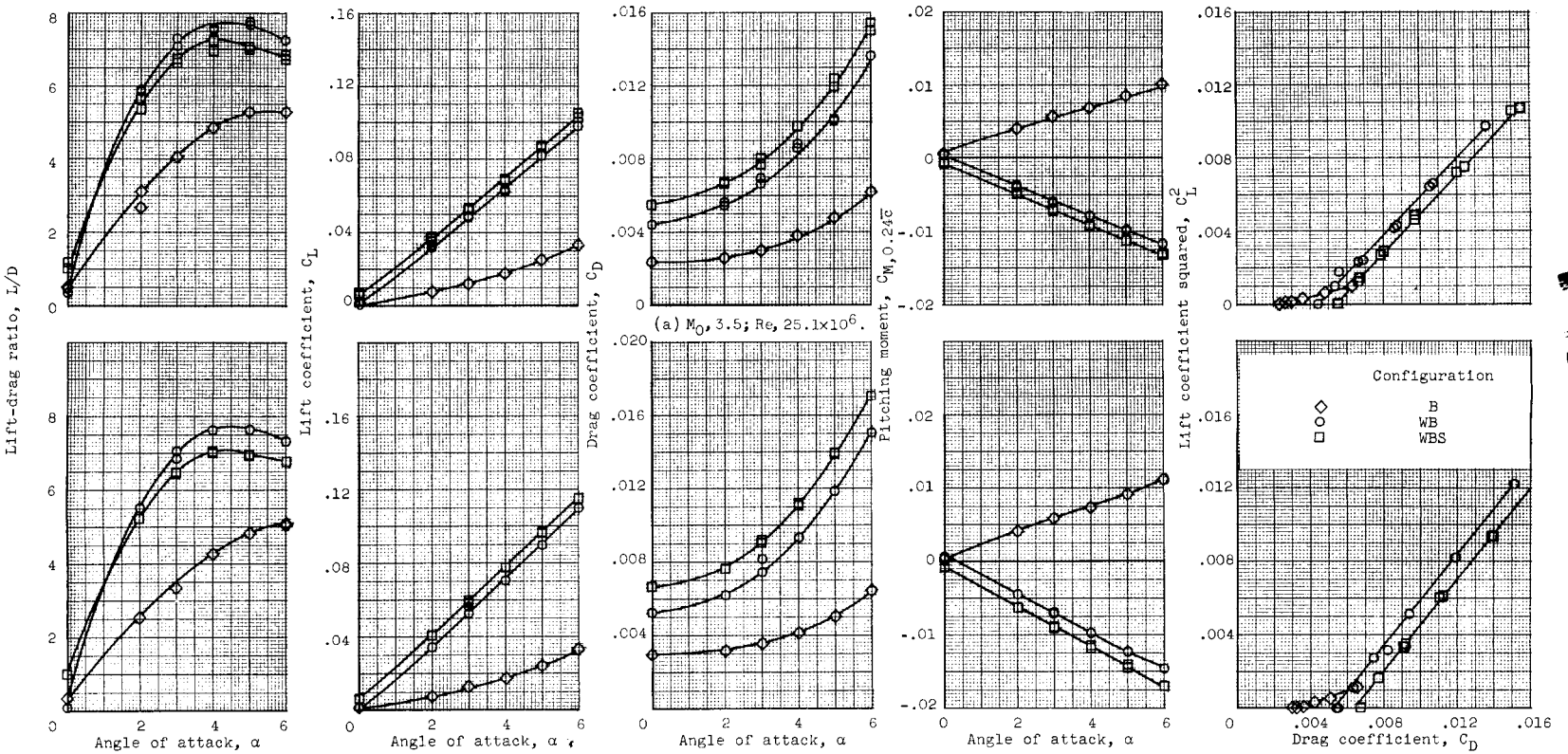


(a) $M_0$, 3.5; Re, $25.1\times10^6$.

(b) $M_0$, 3.0; Re, $19.8\times10^6$.

Figure 3. - Aerodynamic characteristics of flat-bottom configuration without inlet.

DECLASSIFIED

DECLASSIFIED

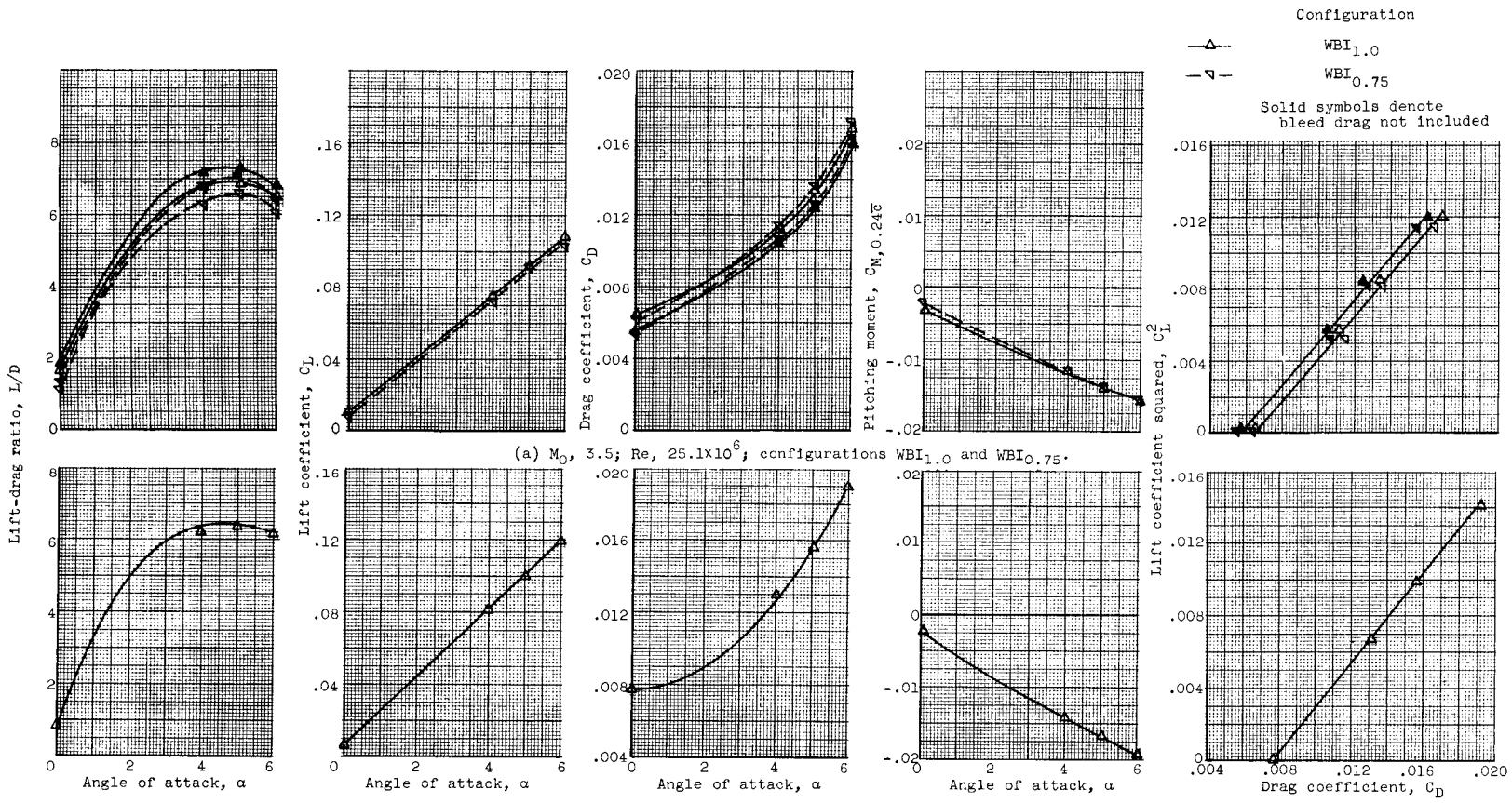


(a) $M_0$, 3.5; Re, $25.1 \times 10^6$; configurations $WBI_{1.0}$ and $WBI_{0.75}$.

(b) $M_0$, 3.0; Re, $19.8 \times 10^6$; configuration $WBI_{1.0}$.

Figure 4. - Aerodynamic characteristics of flat-bottom configuration with inlet installed.

DECLASSIFIED

DECLASSIFIED
CONFIDENTIAL

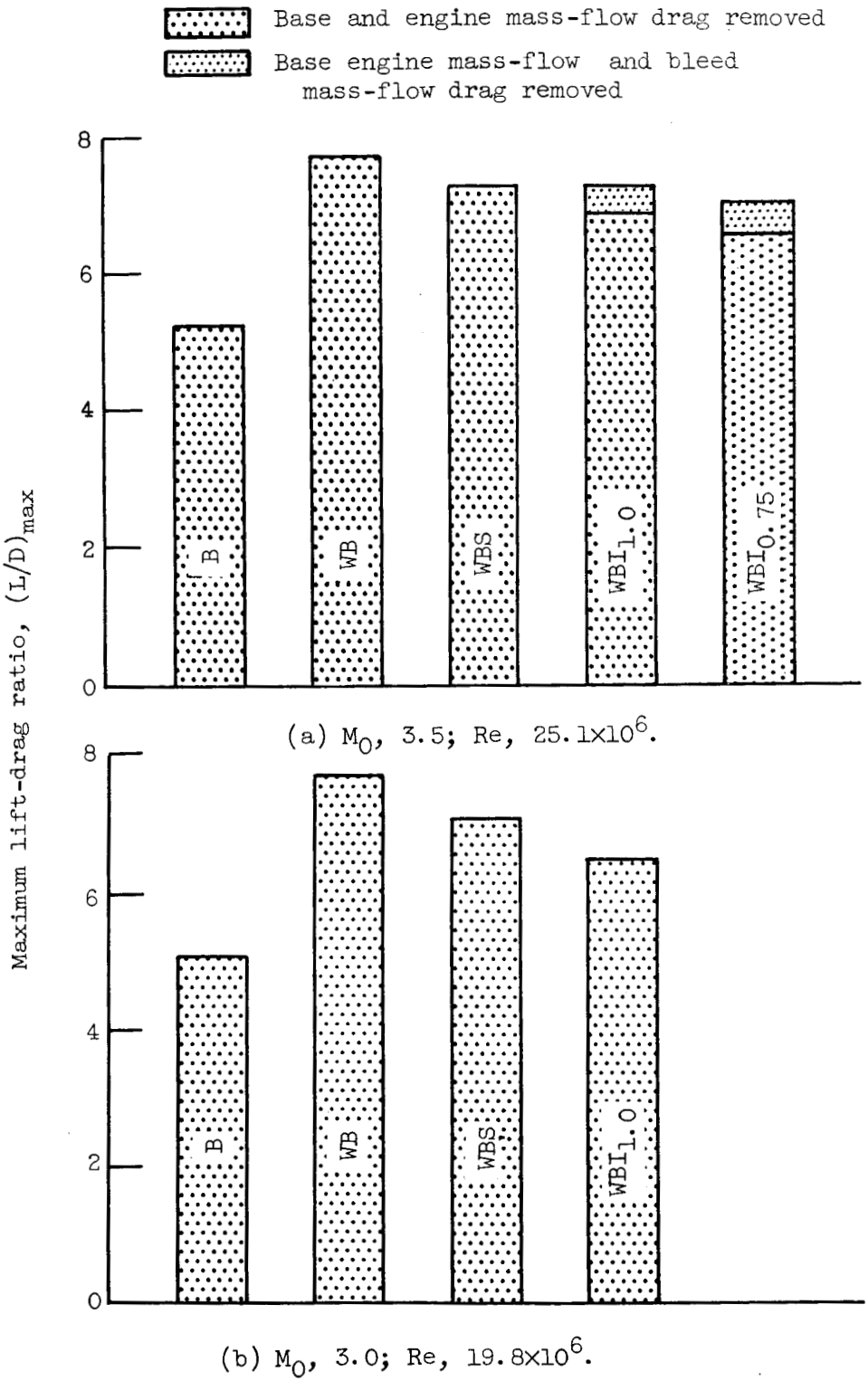


Figure 5. - Comparison of maximum lift-drag ratios for all configurations.

DECLASSIFIED
CONFIDENTIAL

E-722

DECLASSIFIED
CONFIDENTIAL



E-722

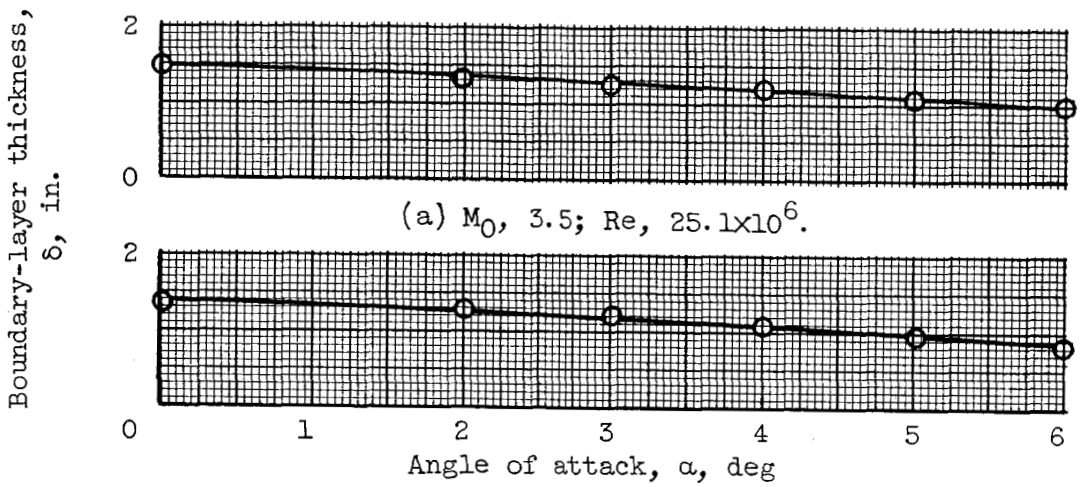


(a) $M_0$, 3.5; Re, $25.1 \times 10^6$.

(b) $M_0$, 3.0; Re, $19.8 \times 10^6$.

Figure 6. - Boundary-layer survey ahead of inlet.

DECLASSIFIED
CONFIDENTIAL

CONFIDENTIAL
DECLASSIFIED

E-722

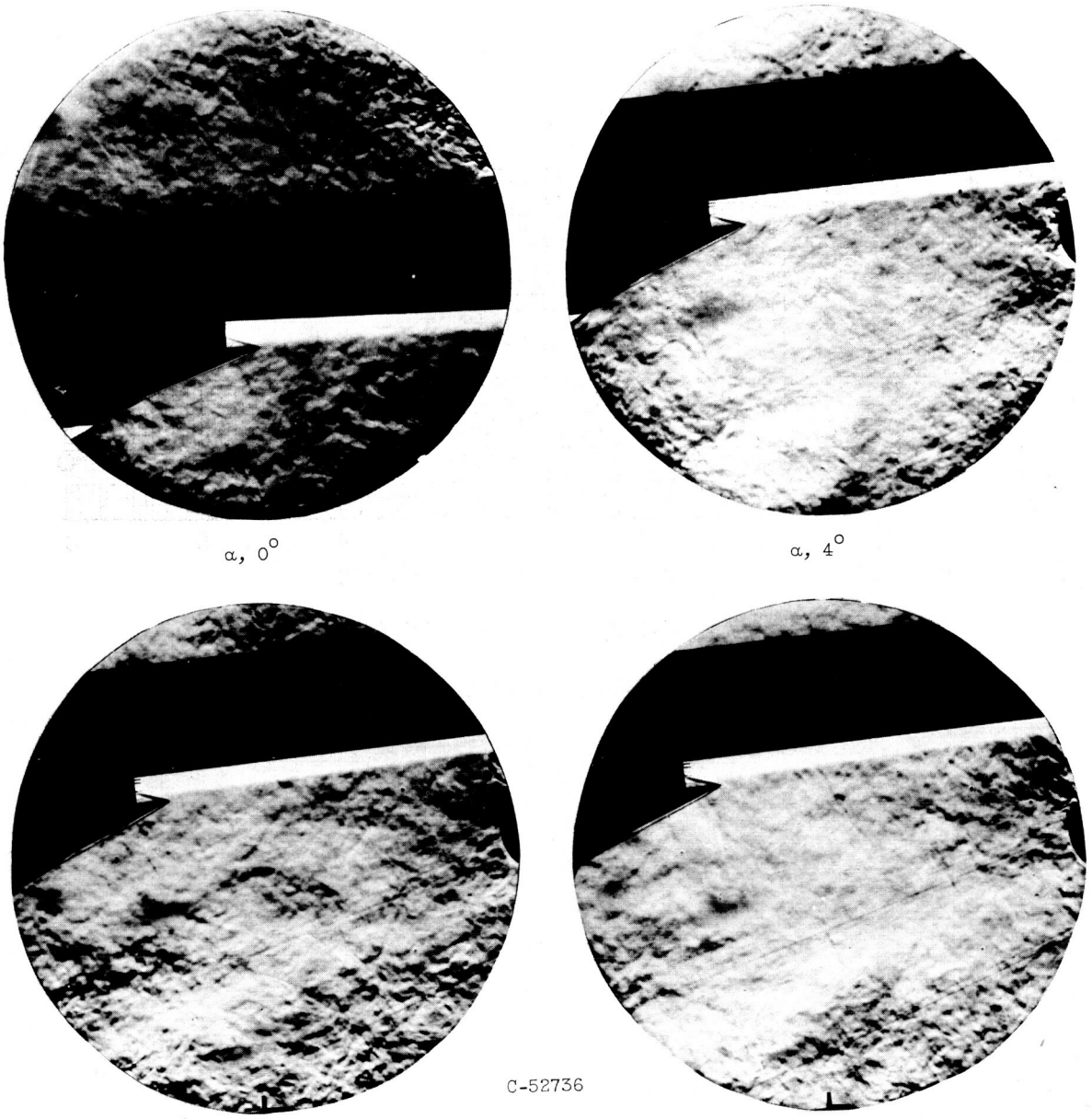


(a) $M_0$, 3.5; Re, $25.1 \times 10^6$.

Figure 7. - Schlieren photographs of critical inlet operation, configuration $WBI_{1.0}$.

DECLASSIFIED
CONFIDENTIAL

DECLASSIFIED


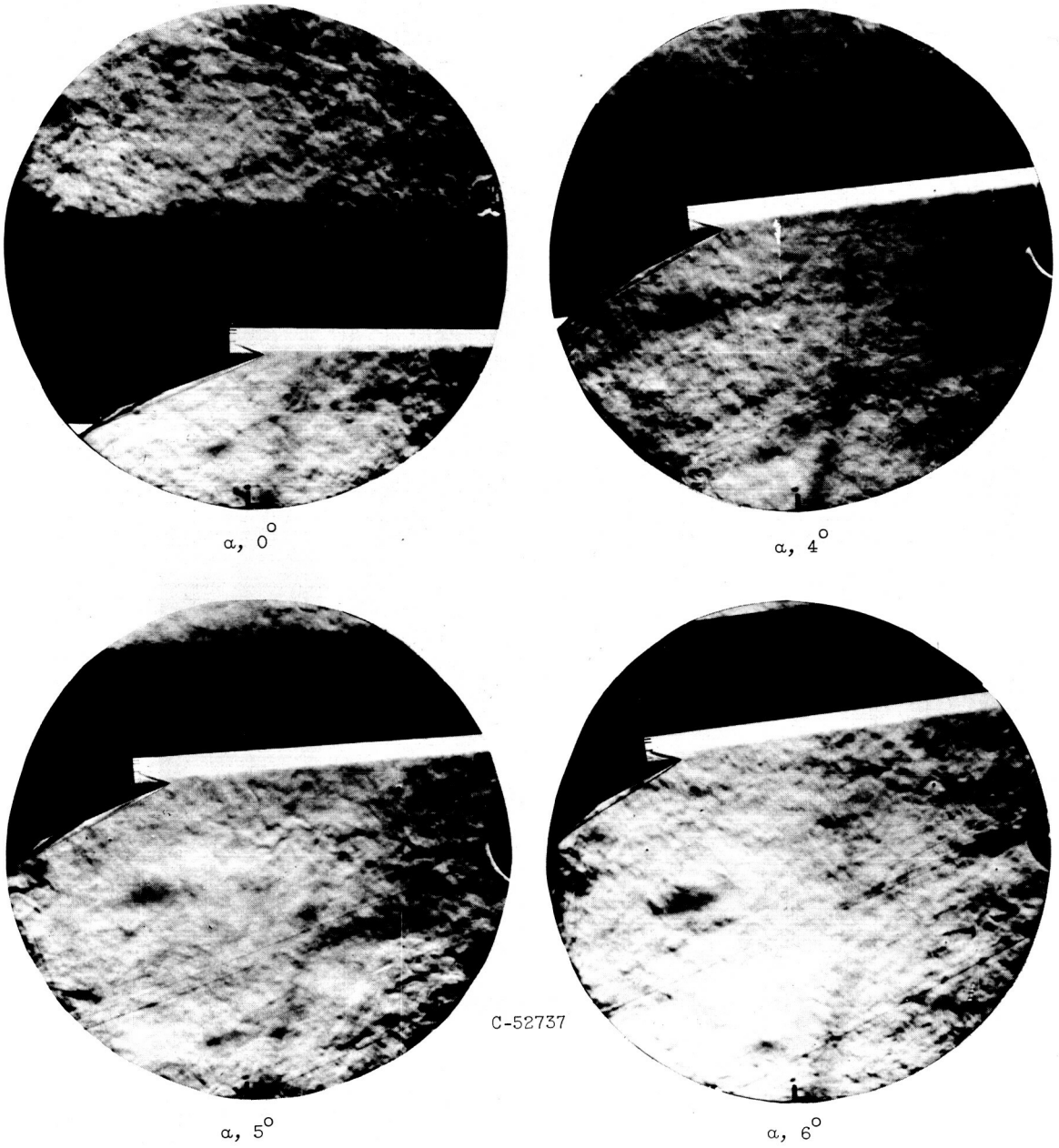


(b) $M_0$, 3.0; Re, $19.8 \times 10^6$.

Figure 7. - Concluded. Schlieren photographs of critical inlet operation, configuration $WBI_{1.0}$.

DECLASSIFIED

DECLASSIFIED
CONFIDENTIAL

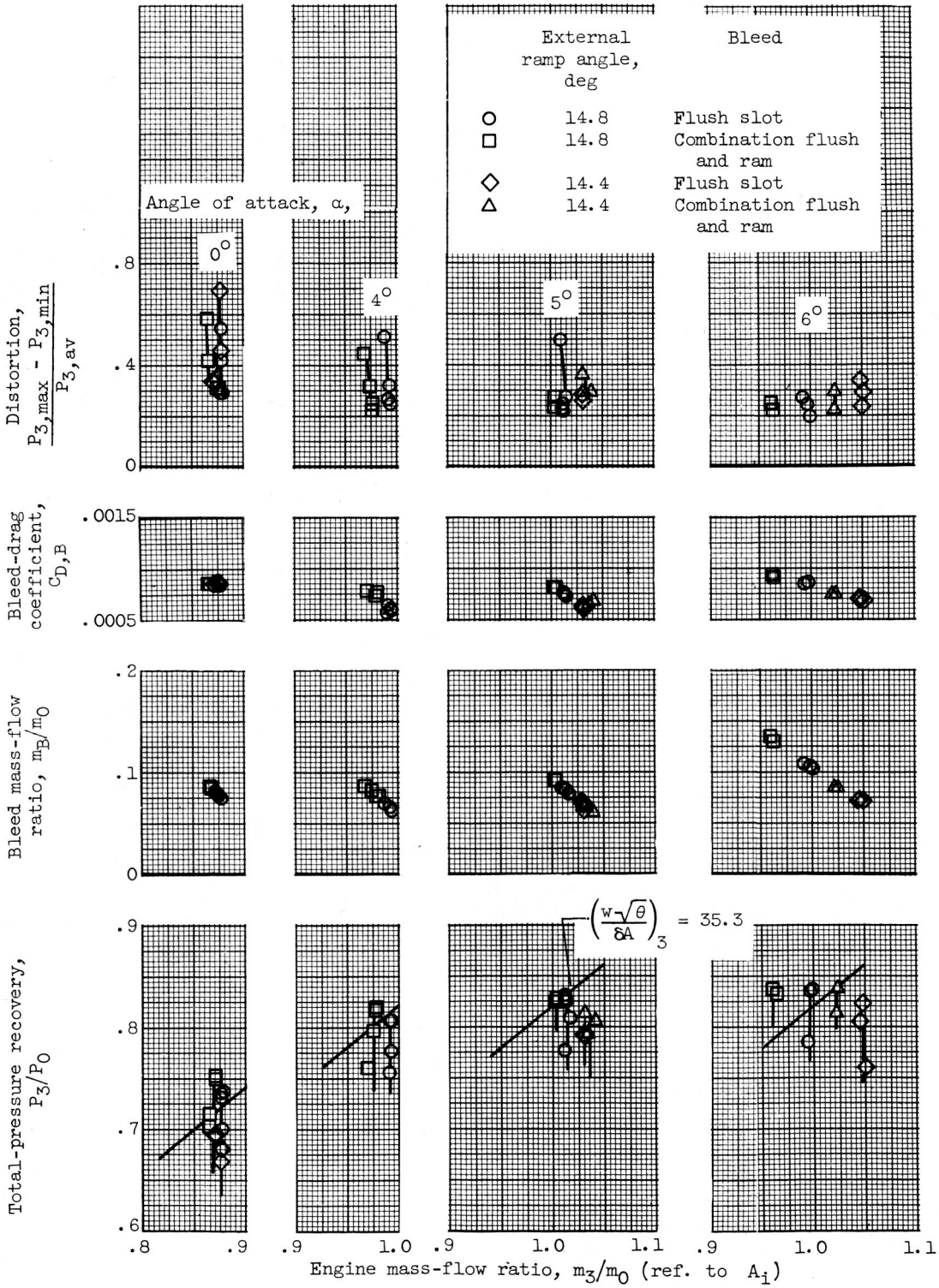


(a) Configuration $WBI_{1.0}$.

Figure 8. - Inlet performance characteristics at free-stream Mach number of 3.5 and Reynolds number of $25.1 \times 10^6$.

CONFIDENTIAL
DECLASSIFIED

DECLASSIFIED



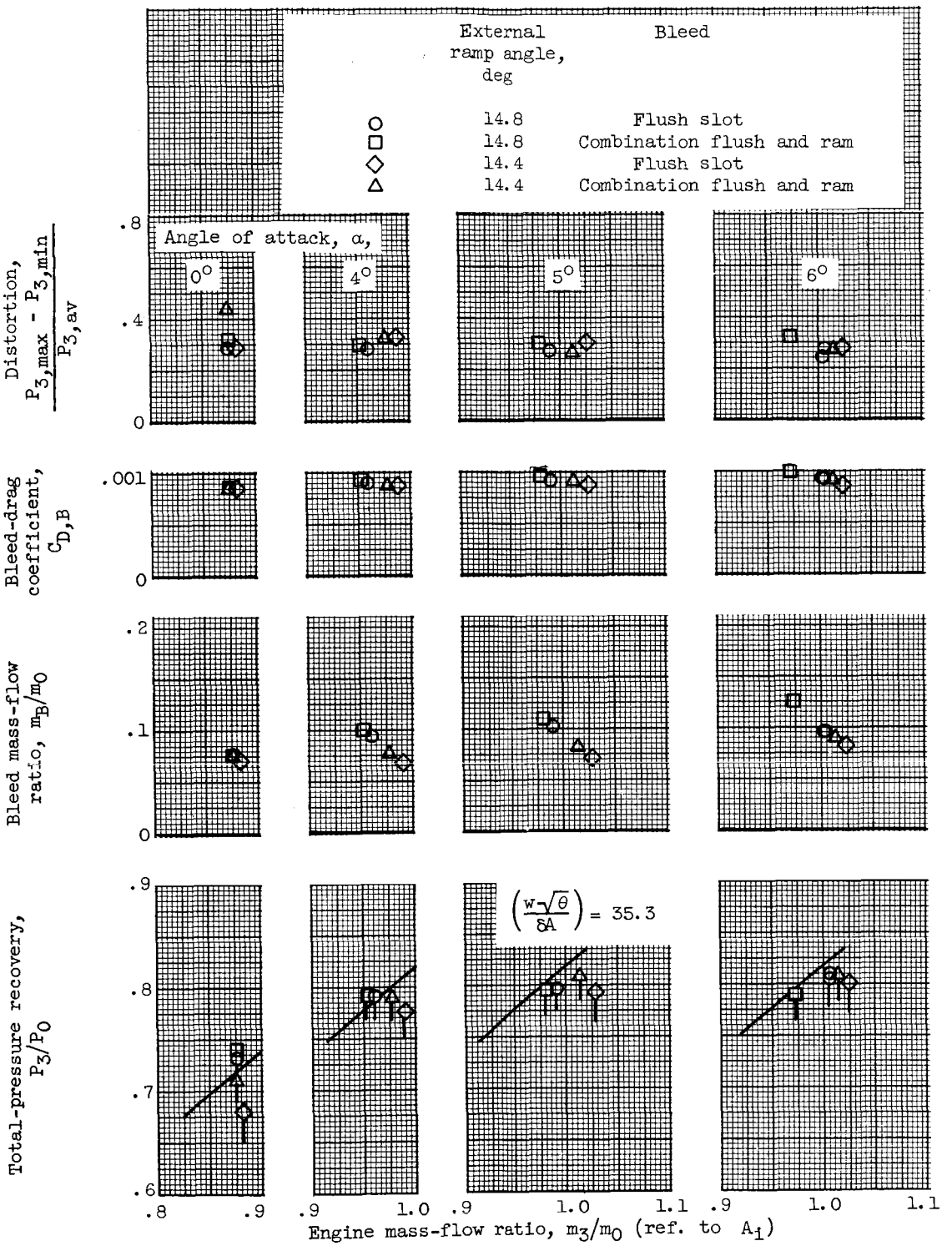


(b) Configuration $WBI_{0.75}$.

Figure 8. - Concluded. Inlet performance characteristics at free-stream Mach number of 3.5 and Reynolds number of $25.1 \times 10^6$.

DECLASSIFIED

DECLASSIFIED

CONFIDENTIAL

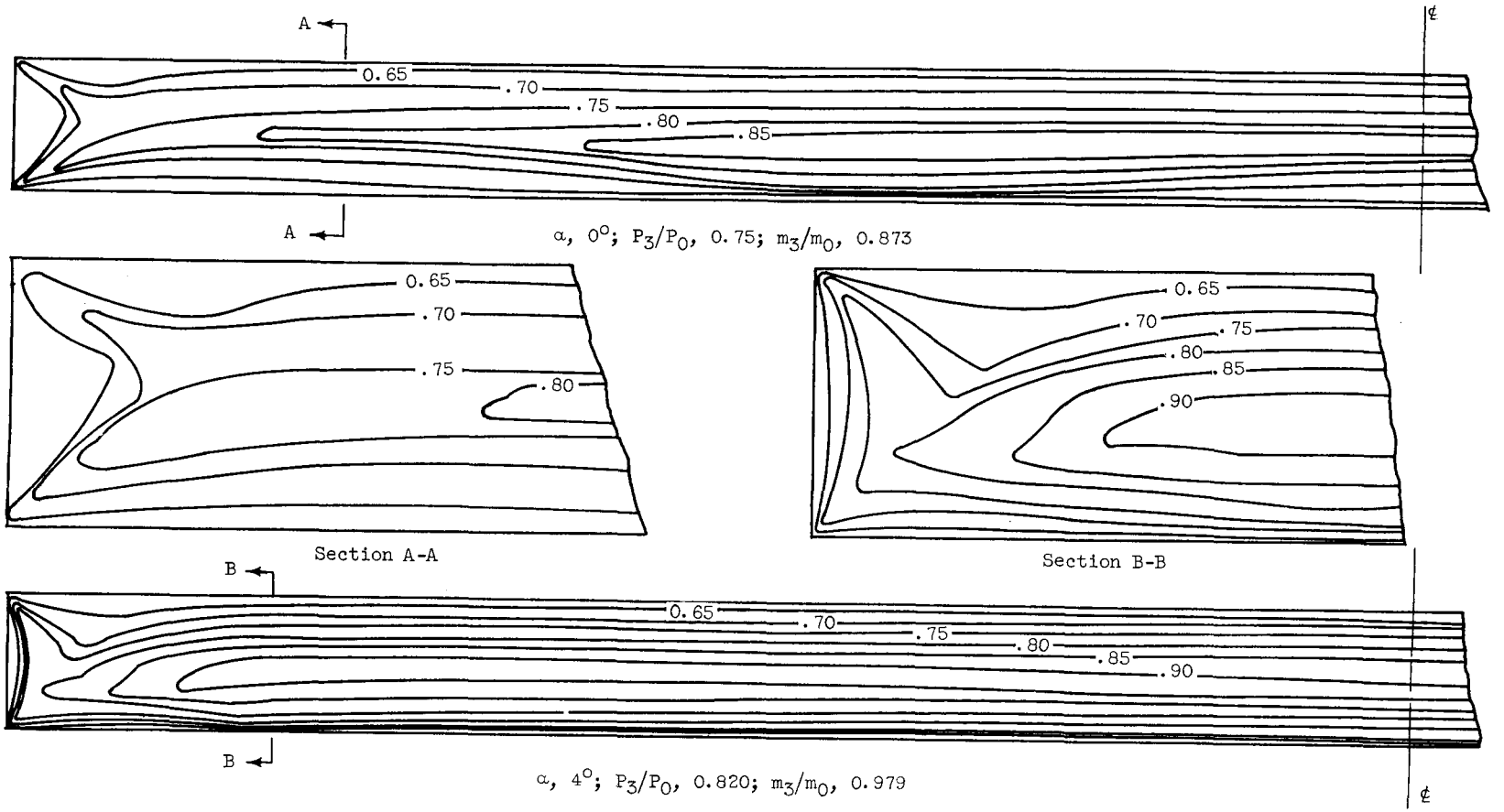


Figure 9. - Compressor-face-station total-pressure contours at critical inlet operation. Free-stream Mach number, 3.5; Reynolds number, $25.1 \times 10^6$; configuration $WBI_{1.0}$.

DECLASSIFIED

E-722

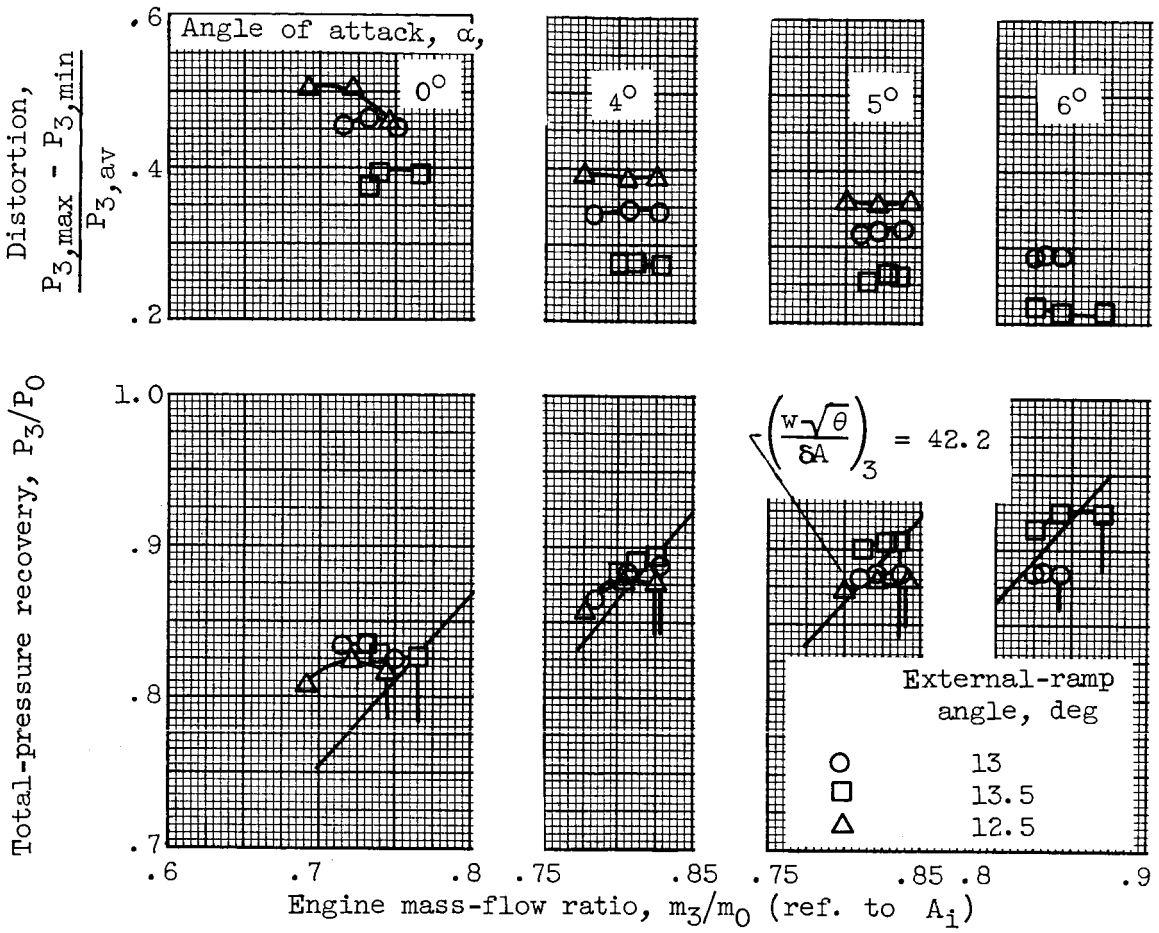


Figure 10. - Performance characteristics of configuration $WBI_{1.0}$ at free-stream Mach number of 3.0 and Reynolds number of $19.8 \times 10^6$.

DECLASSIFIED
CONFIDENTIAL

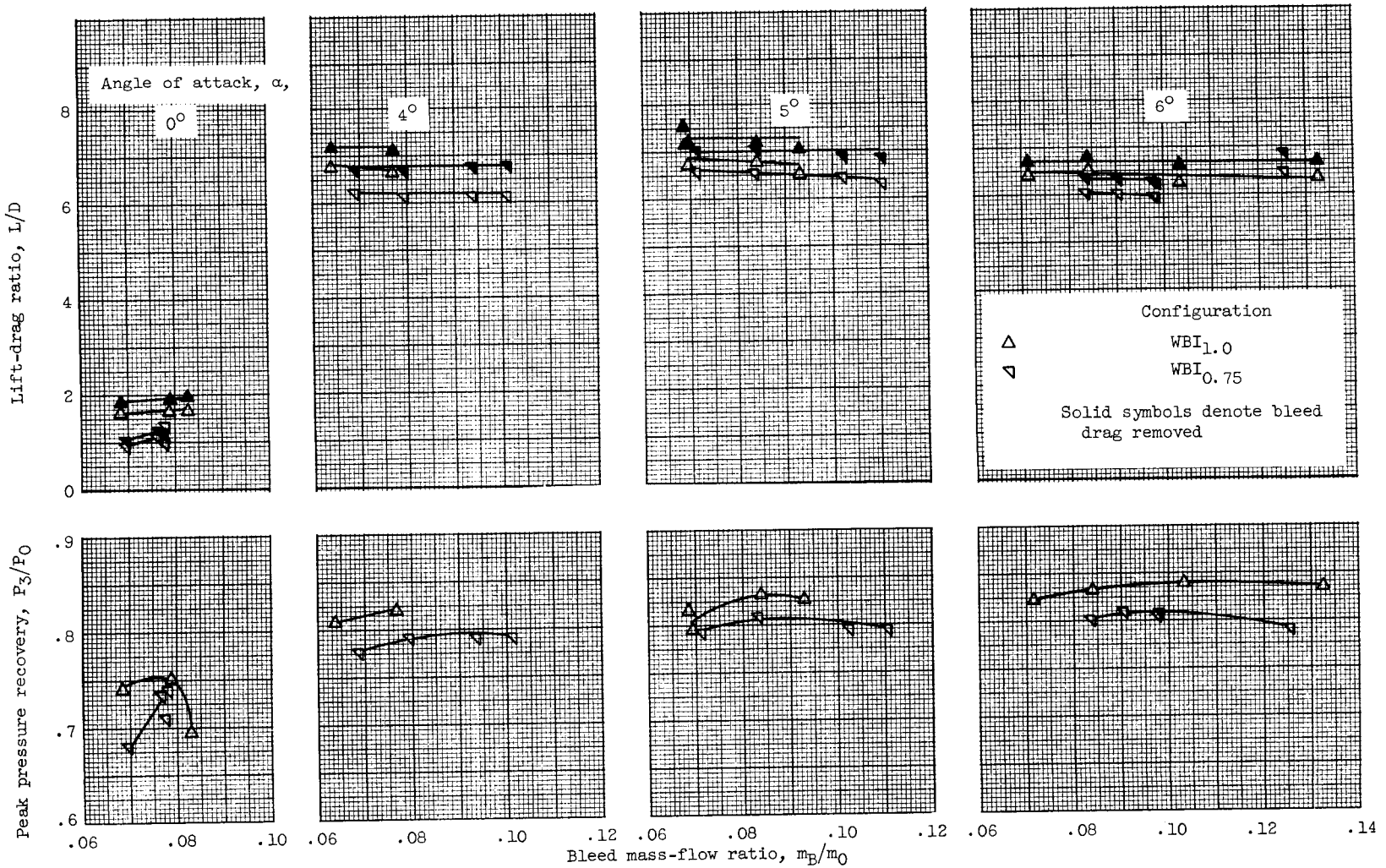


Figure 11. - Effect of bleed mass flow on inlet recovery and configuration lift-drag ratio at free-stream Mach number of 3.5 and Reynolds number of $25.1 \times 10^6$.

DECLASSIFIED
CONFIDENTIAL

DECLASSIFIED
CONFIDENTIAL


E-722

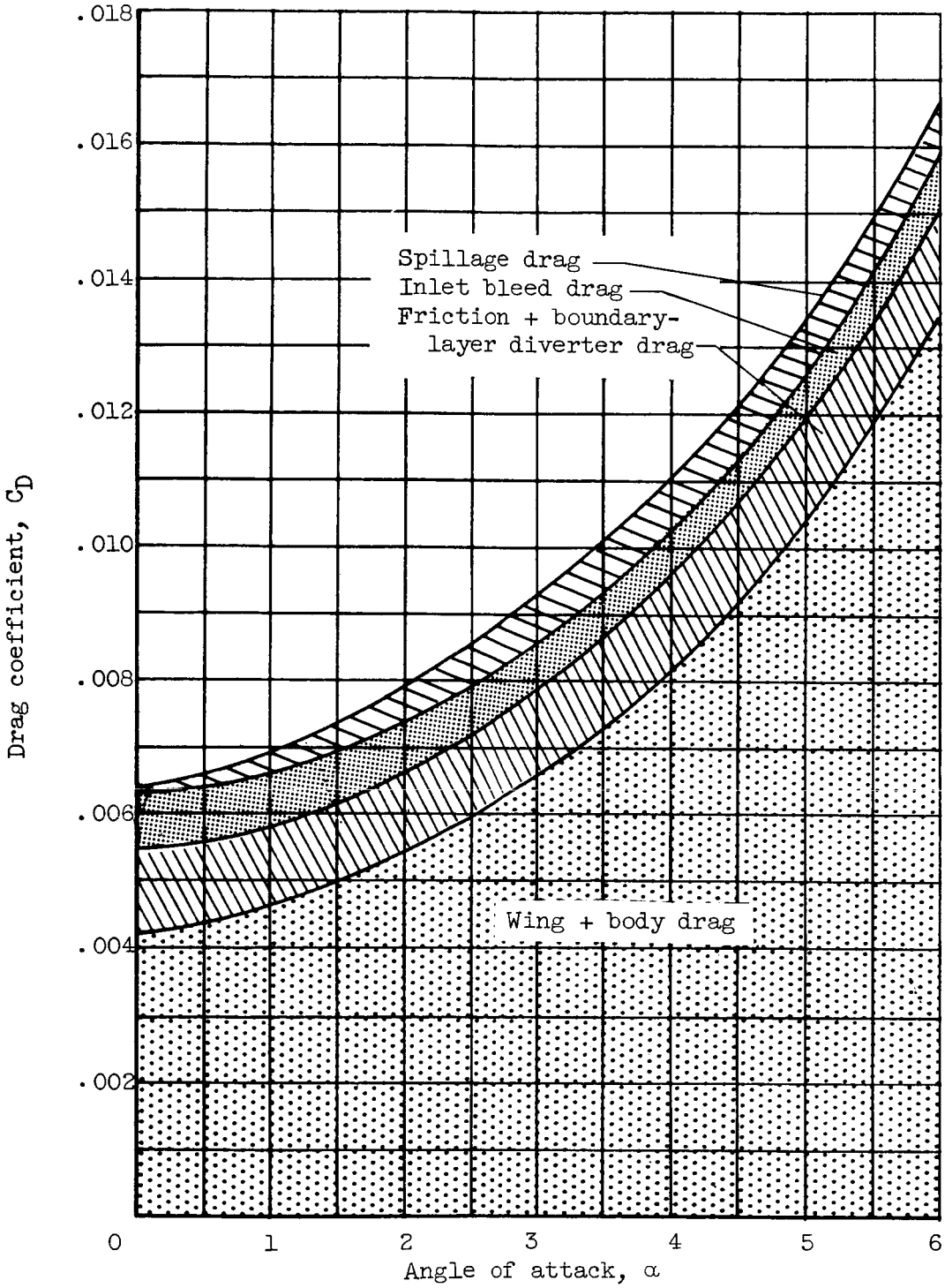


Figure 12. - Component drag values for configuration $WBI_{1.0}$ at free-stream Mach number of 3.5 and Reynolds number of $25.1 \times 10^6$.


DECLASSIFIED
CONFIDENTIAL

CONFIDENTIAL
DECLASSIFIED

NOTES: (1) Reynolds number is based on the diameter of a circle with the same area as that of the capture area of the inlet.

(2) The symbol * denotes the occurrence of buzz.

INLET BIBLIOGRAPHY SHEET

| Report and facility | Description | | | Test parameters | | | | Test data | | | | Performance | | Remarks |
|---|---|---|---|---|---|---|---|---|---|---|---|---|---|---|
| | Configuration | Number of oblique shocks | Type of boundary-layer control | Free-stream Mach number | Reynolds number $\times 10^{-6}$ | Angle of attack, deg | Angle of yaw, deg | Drag | Inlet-flow profile | Discharge-flow profile | Flow picture | Maximum total-pressure recovery | Mass-flow ratio | |
| CONFID. TM X-256 Lewis 10- by 10-ft super-sonic wind tunnel | | Isen-tropic | Ramp flush slot and 4-wall throat bleed | 3.5 and 3.0 | 1.595 and 1.26 | $0^{\circ}$ to $6^{\circ}$ | 0 | √ | | √ | √ | √ | 0.87 to 1.05 | $m_0 = \rho_0 V_0 A_i$ |
| CONFID. TM X-256 Lewis 10- by 10-ft super-sonic wind tunnel | | Isen-tropic | Ramp flush slot and 4-wall throat bleed | 3.5 and 3.0 | 1.595 and 1.26 | $0^{\circ}$ to $6^{\circ}$ | 0 | √ | | √ | √ | √ | 0.87 to 1.05 | $m_0 = \rho_0 V_0 A_i$ |
| CONFID. TM X-256 Lewis 10- by 10-ft super-sonic wind tunnel | | Isen-tropic | Ramp flush slot and 4-wall throat bleed | 3.5 and 3.0 | 1.595 and 1.26 | $0^{\circ}$ to $6^{\circ}$ | 0 | √ | | √ | √ | √ | 0.87 to 1.05 | $m_0 = \rho_0 V_0 A_i$ |
| CONFID. TM X-256 Lewis 10- by 10-ft super-sonic wind tunnel | | Isen-tropic | Ramp flush slot and 4-wall throat bleed | 3.5 and 3.0 | 1.595 and 1.26 | $0^{\circ}$ to $0^{\circ}$ | 0 | √ | | √ | √ | √ | 0.87 to 1.05 | $m_0 = \rho_0 V_0 A_i$ |

Bibliography

NASA-C-8070(2-13-58)

These strips are provided for the convenience of the reader and can be removed from this report to compile a bibliography of NASA inlet reports. This page is being added only to inlet reports and is on a trial basis.

DECLASSIFIED
CONFIDENTIAL